Chapter 10

Stretching continents

The most important isostatic consequence of crustal deformation relates to the changes in the density structure of the lithosphere which dictates the isostatically-supported elevation of the lithosphere. For convergent deformations, involving crustal thickening, the isostatic response is (generally) uplift (or mountain building). For extensional deformations the isostatic effect is in part subsidence (or basin formation) and in part uplift, depending on:

- how the extensional strain is distributed within the lithosphere; and
- whether mantle melts have been added to the lithosphere during extension.

Basins formed as the isostatic consequence of extensional deformations are termed stretch basins and include most continental passive margins formed during continental breakup events.

10.1 Isostatic calculations

Rift Phase Subsidence

The treatment of the isostatic consequences of an extensional deformation is similar to te treatment of the uplift caused by convergent deformation, only now we have also to consider the density distribution of the medium filling the basin. We first consider the effects of a homogeneous extensional deformation on the scale of the lithosphere with no magmatic additions (Figure 11.2):

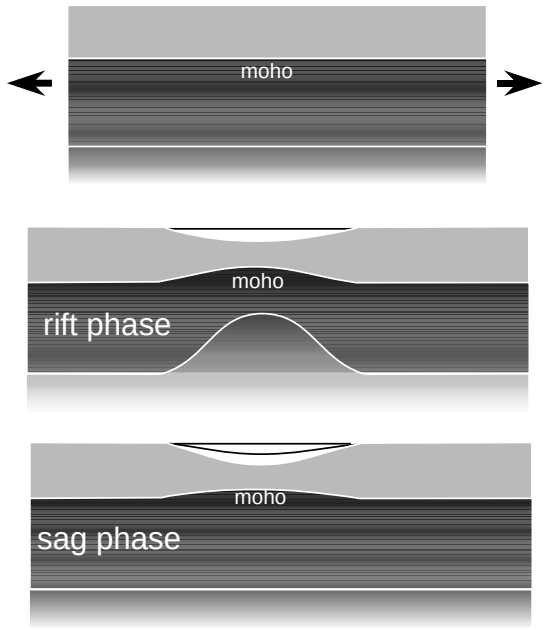

Figure 10.1: Lithospheric-scale extensional geometry used to quantify subsidence.

$$\left(\frac{\partial \dot{\epsilon}_{zz}}{\partial z}\right)_x = 0 \tag{10.1}$$

Using this condition we can parameterize the deformation at any point within the basin in terms of the one dimensional vertical strain:

$$\beta = \frac{1}{\dot{\epsilon}_{zz}} \tag{10.2}$$

Which for plane strain ($\dot{\epsilon}_{yy} = 0$) gives $\beta = \dot{\epsilon}_{xx}$ or, equivalently, the horizontal stretch across the basin. Note that β is the reciprocal of f, the thickening factor used in Chapter 9.

We can formulate the isostatic effects of active rifting in the following manner. Assuming an intial linear lithospheric geotherm, which amounts to ignoring the effects of any internal heat production, gives the temperature T_z at depth z (Figure 10.1) :

$$T_z = T_s + (T_l - T_s)\,\frac{z}{z_l} \qquad 0 < z < z_l \tag{10.3}$$

where T_l is the temperature at the base of the lithosphere, T_s is the temperature at the surface of the lithsophere and z_l is the thickness

of the lithosphere prior to stretching (Figure 10.1). Letting T_m equal the temperature difference across the lithosphere, and setting $T_s = 0$, gives:

$$T_z = T_m \frac{z}{z_l} \qquad 0 < z < z_l \tag{10.4}$$

After homogeneous stretching by a factor β the thermal structure is given by:

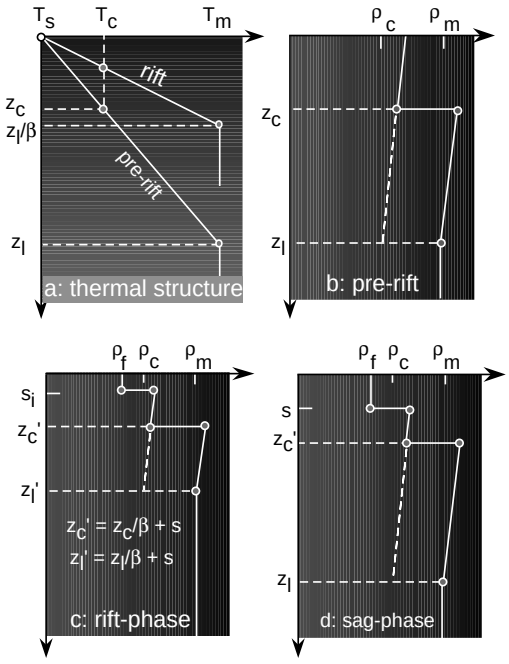

Figure 10.2: Temperature (a) and density (b-d) structure assumed in determining subsidence in a stretched basin. (b) shows denstiy structure prior to stretching, (c) shows density structure immediately after instantaneous stretching, (d) shows density structure after thermal sag.

$$\begin{aligned} T_z &= T_m \, \beta \frac{z}{z_l} \qquad 0 < z < \frac{z_l}{\beta} \\ T_z &= T_m \qquad \frac{z_l}{\beta} < z < z_l \end{aligned} \tag{10.5}$$

The initial vertical density structure is given by (Figure 10.1):

$$\rho_z = \rho_c \left(1 + \alpha \, T_m \left(1 - \frac{z}{z_l}\right)\right) \qquad 0 < z < z_c$$

$$\rho_z = \rho_m \left(1 + \alpha\, T_m \left(1 - \frac{z}{z_l}\right)\right) \qquad z_c < z < z_l \tag{10.6}$$

where ρ_c and ρ_m are respectively, the density of the crust and mantle at the temperature T_m and α is the volumetric coefficient of thermal expansion. Following stretching by β the density structure is:

$$\begin{aligned}
\rho_z &= \rho_f && 0 < z < S_i \\
\rho_z &= \rho_c \left(1 + \alpha\, T_m \left(1 - \frac{z\,\beta}{z_l}\right)\right) && S_i < z < Si + \tfrac{z_c}{\beta} \\
\rho_z &= \rho_m \left(1 + \alpha\, T_m \left(1 - \frac{z\,\beta}{z_l}\right)\right) && S_i + \tfrac{z_c}{\beta} < z < S_i + \tfrac{z_l}{\beta} \\
\rho_z &= \rho_m && S_i + \tfrac{z_l}{\beta} < z < z_l
\end{aligned} \tag{10.7}$$

where ρ_f is the density of the medium filling the rift basin of thickness S_i. The condition of isostasy amounts to equating the vertical stress, σ_{zz}, at a common depth, z_l, beneath the unstretched and stretched basin. Beneath the unstretched lithosphere σ_{zz} at z_l is given by (allowing that $\rho_c\,\alpha_c = \rho_m\,\alpha_m$):

$$\begin{aligned}
\sigma_{zz}\,|_{z=z_l} &= g \int_0^{z_l} \rho_z\, dz \\
&= g\, z_c\, \rho_c + g(z_l - z_c)\rho_m + \frac{z_l}{2}\, g\, \alpha\, \rho_m\, T_m
\end{aligned} \tag{10.8}$$

Beneath the stretched basin σ_{zz} at z_l is given by:

$$\begin{aligned}
\sigma_{zz}\,|_{z=z_l} &= g \int_0^{z_l} \rho_z\, dz \\
&= g\, \rho_f\, S_i + g\, z_c\, \rho_c\, \beta + g\, (z_l - z_c)\rho_m \beta \\
&\quad + \frac{g\, z_l\, \alpha\, \rho_m T_m}{2\beta} + g\, \rho_m \left(z_l - S_i - \frac{z_l}{\beta}\right)
\end{aligned} \tag{10.9}$$

equating Eqn 10.8 with Eqn 10.9 and solving for S_i gives (Figure 10.1):

$$S_i = (\beta - 1)\ (2\, z_c\, (\rho_c - \rho_m)\ + T_m\, \alpha\, z_l\, \rho_m\,)\, 2\, \beta\ (\rho_f - \rho_m) \tag{10.10}$$

Sag Phase Subsidence

We assume that in the steady state the thickness of the lithosphere is dictated by balancing the rate of heat flow through the lithosphere

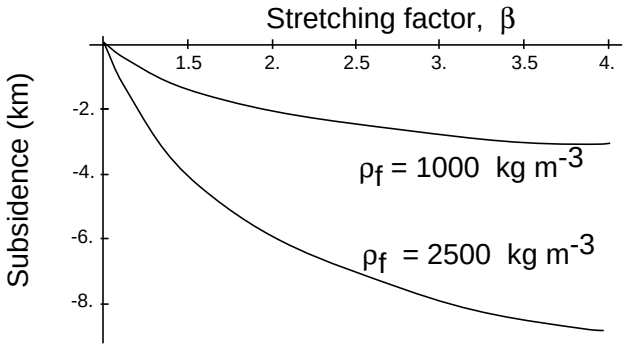

Figure 10.3: Rift phase subsidence as a function of stretching for a basin completely filled by sediment ($\rho_f = 2500$ kg m^{-3}), and water ($\rho_f = 1000$ kg m^{-3}).

with the heat supplied to its base by the convective motion in the interior. Any deformation involving changes in the thickness of the lithosphere therefore induces a departure from this equilibrium condition which in turn influences the ensuing thermal evolution of the lithosphere. Since heat loss is proportional to the temperature gradient in the lithosphere extensional deformation brings the asthenosphere closer to the surface and consequently increases the heat loss through the lithosphere (Chapter 4). This imbalance causes heat to be lost through the lithosphere more quickly than it is supplied. The consequent cooling and thickening of the lithosphere causes it to become more dense, inducing a kind of thermal subsidence or sag. There are two questions of interest here:

- what is the relationship between the stretching factor β and the induced thermal subsidence; and
- over what time scale does the thermal subsidence take place (this question will be addressed in Section 10.4).

We can formulate the isostatic effects of the thermal or sag phase subsidence, S_t, following a stretching by a factor β in the following manner. Following reestablishment of the equilibrium lithospheric thickness, z_l, by conductive heat loss the density distribution will be:

$$\rho_z = \rho_f \qquad 0 < z < S_t + S_i$$

$$\rho_z = \rho_c \left(1 + \alpha\, T_m \left(1 - \frac{z}{z_l}\right)\right) \qquad S_t + S_i < z < S_t + S_i + \frac{z_c}{\beta}$$
$$\rho_z = \rho_m \left(1 + \alpha\, T_m \left(1 - \frac{z}{z_l}\right)\right) \qquad S_t + S_i + \frac{z_c}{\beta} < z < z_l \quad (10.11)$$

where S_t is the subsidence due to thermal sag. Letting the total subsidence, $S = S_t + S_i$, then σ_{zz} at z_l beneath the saged basin is given by:

$$\begin{aligned} \sigma_{zz}|_{z=z_l} &= g \int_0^{z_l} \rho_z \, dz \\ &= g\, \rho_f\, S + g\, z_c\, \rho_c\, \beta + \\ &\quad g\, \rho_m \left(z_l - S - \frac{z_c}{\beta} + \frac{z_l\, \alpha\, T_m}{2}\right) \end{aligned} \quad (10.12)$$

Solving for S gives:

$$S = \frac{z_c(\beta - 1)\,(\rho_c - \rho_m))}{\beta\,(\rho_f - \rho_m)} \quad (10.13)$$

and S_t (Figure 10.1):

$$S_t = \frac{T_m\, \alpha\, \rho_m\, z_l\ (\beta - 1)}{2\,\beta\,(\rho_f - \rho_m)} \quad (10.14)$$

Heterogeneous stretching of the lithosphere

The $f_c - f_l$ diagrams (note that f is the reciprocal of β) shown in Figure 10.1 allows the rift phase subsidence to be calculated for any inhomogeneous stretching deformation, in which the deformation is not equally partitioned between the crust and mantle (although in these diagrams there has been no allowance made of the density of the medium filling the depressions). The $f_c - f_l$ parameterisation allows us to consider the isostatic effects of magma additions to the crust during extension, as for instance has occurred during stretching of the Basin and Range Province in the western USA. Magma additions add mass to the crust, with the result that $f_c > f_l$. In the Basin and Range Province magma addition appears to have been sufficent to maintain a crustal thickness in the vicinity of 30 km, while the underlying mantle part of the lithosphere has been severely attenuated (Gans, 1988). The resulting path shown in Figure 10.1 explains the anomalously high elevation of the Basin and Range Province. Finally, the isostatic effects of stretching are dependent to a large

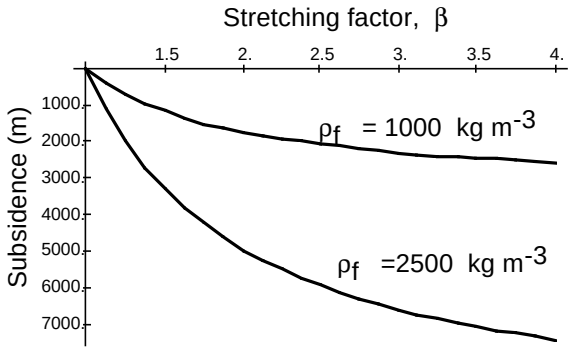

Figure 10.4: Sag phase subsidence as a function of stretching for a basin completely filled by sediment ($\rho_f = 2500$ kg m^{-3}), and water ($\rho_f = 1000$ kg m^{-3})

extent on the vertical density structure of the lithosphere prior to stretching. For typical continental lithosphere we have shown that homogeneous (or pure shear) thinning results in subsidence. In contrast, Figure 10.1 shows that homogeneous thinning of old oceanic lithosphere results in uplift or Ridge formation. Indeed, this is exactly as we showed in Chapter 7, and this is exactly why the ocean ridges are important engines for lithospheric motion and deformation.

10.2 Mechanical consequences of extension

Inttroduction

So far we have treated basin formation in terms of a kinematic model only, that is without consideration of the forces that drive the deformation. In order to develop a mechanical model we must consider the thermal evolution of stretch basins explicitly, because the mechanical strength of the lithosphere is closely allied to its thermal state. We use the mechanical model described in Chapter 2.

The time scale of thermal sag

As discussed in Chapter 4.3 a convenient measure of the response time to thermal perturbations in media in which heat is transported

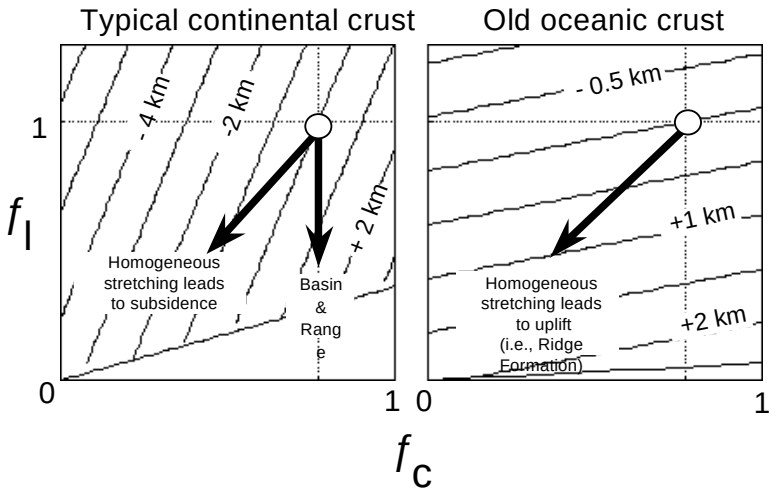

Figure 10.5: $f_c - f_l$ diagrams for stretching of typical continental lithosphere (z_c = 35 km, z_l = 125 km, elevation contours in 1 km intervals) and typical oceanic crust (z_c = 6 km, z_l = 125 km, elevation contours in 0.5 km intervals). Note that homogeneous stretching of continental lithosphere leads to subsidence (elevation contours for subsidence assume no sedimentation or water filling, to change to a filled basin multiply subsidence by $\rho_m/(\rho_m - \rho_f)$) while homogeneous stretching of oceans leads to uplift (i.e., ridge formations).

only by conduction is given by the thermal time constant, t:

$$\tau = \frac{l^2}{\pi^2 \kappa} \tag{10.15}$$

where l is the length scale over which the perturbation occurs, κ is the thermal diffusivity (units $m^2\ s^{-1}$). The thermal time constant provides a measure of time for the decay of approximately 50% of the thermal perturbation, with measurable deacy occuring up until about 3 τ. The thermal time constant of the continental lithosphere is of the order of 60 Ma ($\kappa = 10^{-6}$ $m^2 s^{-1}$, $l = 10^5$ m), and thus we may expect that subsidence associated with sag of a rifted basin for a period of up to 150-200 Ma (Figure 10.2).

Since the decay of a thermal perturbation is proportional to the second derivative of the temperature gradient with respect to depth (Chapter 4) and is therefore an exponentially decreasing function of time. Consequently, the thermal sag subsidence should also decline exponentially with time.

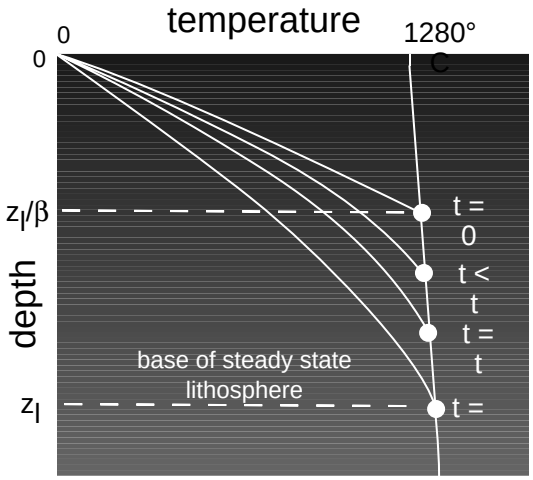

Figure 10.6: Evolution of the geotherm during sag following instantaneous stretching at time $t = 0$.

Thermal evolution at finite extensional strain rates

The instantaneous thinning of lithosphere will result in isothermal decompression of all material points in the lithosphere. The resultant increase in the geotherm for an instantaneous stretch is β. However, lithosphere stretched at finite rates will evolve geotherms lower than the theoretical "instantaneous" geotherm for two reasons. with important consequence for the evolution of strength within the lithosphere .

note that we were able to ignore these thermal effects in our analysis of subsidence presented in sections 9.2 and 9.3 because we assumed an instantaneous stretch

- Firstly any stretching event will necessarily cause the vertically integrated volumetric heat production of the lithosphere to diminish (by a factor of β for homogenous stretching events). Assuming a steady state geotherm prior to stretching then the declining heat production caused by stretching will lead to cooling of individual material points within the lithosphere (Figure 10.2), with the amount of cooling for a given stretch inversely proportional to the strain rate.

- Secondly, lithosphere stretched at finite rates will evolve geotherms lower than the theoretical "instantaneous" geotherm because

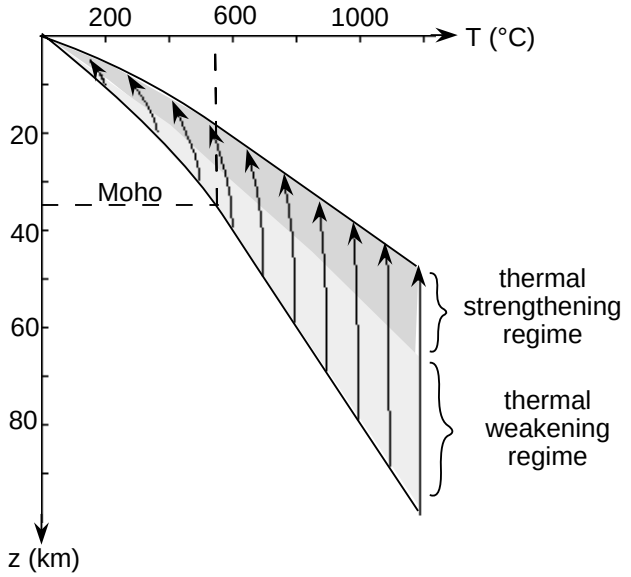

Figure 10.7: Stretching leads to an upward migration of isotherms, and thus an increase in the geotherm. However, for finite stretching rates individual material points cool (as shown by arrowed lines), because the stretching reduces the heat production in any vertical column through the lithosphere by the factor β (the cooling is most pronounced in the crust where most of te heat producing elements reside). This model shows the homogeneous stretching of a 100 km thick lithosphere by $\beta = 2.0$ over 30 Ma ($\dot{\epsilon}_z = 2x10^{-15}$ s^{-1}).

the processes of rifting and sag will overlap in time and space. The extent of overlap will depend on the both the strain rate and the finite strain.

Mechanical Evolution

We have shown that convergent deformation of the continental lithosphere induces weakening due largely to the increase of the Moho temperature associated with increasing heat production within the lithosphere. This provides a self localising mechanism for convergent orogens, with the length scales dictated by the rheology, strain rate relationship. Similarly the length scales for divergent deformation will be also controlled by rheology. The lithosphere is, however, weaker in tension than in compression because brittle failure in tension occurs at lower stress difference than in compression (Figure 10.2). Cconsequenlty, for an equivalent geotherm and strain rate the across strike length scale of an extensional orogen will be significantly

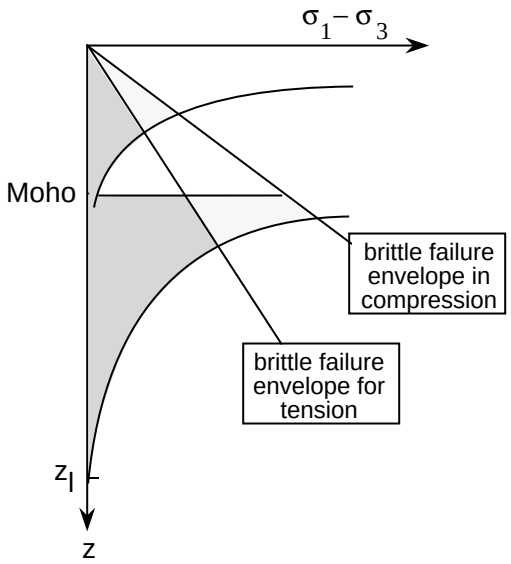

Figure 10.8: See text for discussion

less than a compressional orogen.

For small initial finite stretches the lithosphere will undergo essentially isothermal decompression (Figure 10.2). The consequent decrease in the depth of the power law failure envelopes for quartz and olivine will induce a reduction in the strength of the lithosphere; a form of thermal weakening (Figure 10.2a). However, with increasingly large finite strains, the cooling of material points as they are decompressed (Figure 10.2) ultimately leads to an increase in whole lithospheric strength (Figure 10.2). This analysis suggests that early in their evolution rift zones should be self-localising but gradually becoming more distributed. The point at which the switch from *weakening* to *strengthening* occurs depends critically on the strain rate with the critical strain decreasing with decreasing strain rate.

The role of magmas

Of course the thermal and mechanical evolution of extensional orogens is depenedent not only on the rate of deformation but also on the involvement of asthenospheric magmatic additions. Decompression of the asthenosphere beneath stretched lithosphere may induce melting in an analogous fashion to melting beneath ridges. For the

normal potential temperature of the asthenosphere (1280°C) this requires decompression of asthenosphere beneath depths of approximately 45 km. Assuming initial lithospheric thicknesses of the order of 100 km or more the minimum β value required for melting of the mantle beneath the stretched lithsophere is about 2. Once melting occurs, the rapid advection of heat into the overlying lithosphere will cause dramatic strength reductions, potentially overriding the strain hardening associated with large strains mentioned in the previous section. Moreover, the isostatic consequences of magma addition are to increase the elevation of the lithosphere, as is the case in the Basin and Range Province, potentially giving rise to extensional buoyancy forces which augment the original driving forces for stretching. This magmatically augmented weakening may be an essential requirement for the complete rupturing of stretched continental lithosphere to form new spreading oceans.

The role of mantle plumes

In the discussion above we have not explicitly considered the origin of the forces that drive extension of the continental lithosphere. While it is clear that compressional forces within the continents can be generated by the tractions exerted by subducting slabs it is not at all clear that substantial extensional force may be exerted on normal thickness continetal lithosphere. This is because normal thickness lithosphere (35 km thick crust and 125 km thick lithosphere) is in approximate potential energy balance with the mid-ocean ridges; that is the ridges seem to neither exert compression nor tension on normal continental lithosphere. Of course regions of elevated topography within the continents, such as associated with thickened crust formed in zones of compression, will naturally experience tension when the forces driving convergence are relaxed. Another important way of increasing the potential energy of the lithosphere may be through the impingement of a mantle plume at the base of the lithosphere, which may have the effect of jacking up the lithosphere by as much as 1 km. The associated potential energy gain (for a column of unit area) is given to a first approximation by:

$$U_{plume} = \frac{g\,\rho_c\,h^2}{2} \tag{10.16}$$

where h is the additional elevation caused by the jacking effect of the mantle plume, and for crustal density $\rho_c = 2800$ kg m^{-3} is equivalent

to a tensional force per unit length of topography of about 1.4 x 10^{12} N m^{-1} for every km of additional elevation.

An important additional effect of extension initiated by a plume relates to the higher mantle temperatures which may be up to about 300^{o}C higher than the mean convective mantle temperatures. The implication is that decompression melting in the asthenosphere will begin at a much earlier stage in the rifting process. For example for a potential mantle temperature of 1580^{o}C melting begins at about 120 km depth, implying that plumes may begin generating melts without any appreciable deformation of the overlying lithosphere. Moreover as mentioned in the previous section the transport of such melts into the lithosphere must further enhance the potential energy of the lithosphere and weakens it in such a way to augment any extensional deformation that has already begun.

10.3 Sedimentation in stretched basins

We have seen that the evolution of rift basins can be viewed in terms of two distinct phases: the rift phase, and the sag phase. In the the rift phase sedimentation is associated with the isostatic subsidence induced by the active deformation. Rift phase sediments show signs of active tectonism, such as growth faults with rapid facies and thickness changes. Sag phase sedimentation follows rift phase and represents the isostatic effects of freezing asthenosphere onto the base of the thinned lithosphere as the geotherm returns to steady state. Sag-phase sediments are typically laterally extensive without abrupt facies changes. Subsidence rates decrease exponentially through the sag phase with a characteristic time scale indicative of the thermal time constant of the lithosphere.

The Steer's Head

Stretched basin stratigraphy commonly exhibits a Steer's Head or Texas Longhorn shape with the sag phase sediments extending beyond the zone of observable crustal stretching (Figure 8.9). This characteristic stratigraphy may be a function of either the finite flexural rigidity of the lithosphere or by differential stretching of the crust and mantle parts of the lithosphere (White & Mckenzie, 1988).

In the calculations above we made the simplyfying assumption that the lithosphere is everywhere in local isostatic equilibrium. This

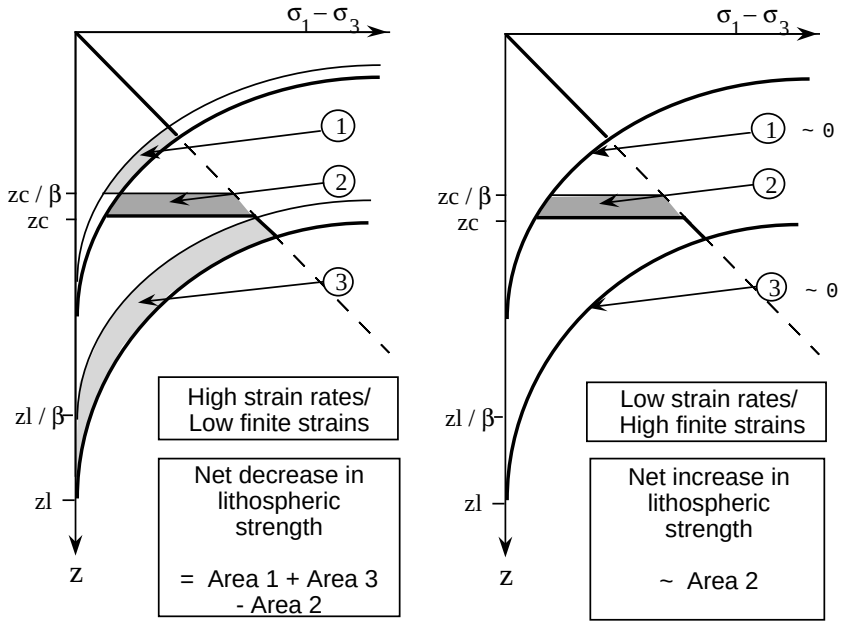

Figure 10.9: Schematic representation of how lithospheric strength changes as a function of stretching. For low finite strains and/or high strain rates decompression is essentially isothermal and thus the plastic failure envelopes move to shallower depths (since they are dependent on temperature and thus only indirectly on depth through the geotherm - Eqn 5.2) inducing a reduction in lithospheric strength by an amount equal to Area 1 + Area 3. A decrease in the depth of the Moho results in a strength increase by an amount equivalent to Area 2. The net change in the lithospheric strength is given by Area 1 + Area 3 - Area 2. At low strain rates and/or high finite strains cooling of material points occurs such that there is no rise in the plastic failure envelopes with further deformation (i.e., Area 1 and Area 3 tend to 0).The consequent strain hardening is equivalent to Area 2. White and McKenzie (1989) point out that in mantle upwelling zones the temperatures may be in excess of 100°C above the typical potential temperature of the mantle. Stretching above such abnormally hot asthenosphere will induce melting at rather lower b values than for normal mantle, and for a given b value contribute a much greater amount of melt to the overlying lithsophere. The variable magmatic history of extensioanl provibnces and rifted margins may therefore relate to the thermal state of the subjacent convective interior during rifting.

amounts to treating the lithosphere as infinitely weak (to vertical shearing) and therefore incapable of supporting bending or flexural stresses. The lithosphere is not infinitely weak but rather has a finite flexural rigidity. The consequences of the finite flexural rigidity are that loads on the lithosphere, such as sedimentary or tectonic loads, are generally compensated on a regional scale rather than a local scale, with significant local departures from isostatic equilibrium. In the case of the deposition of sediment in rift basins the finite flexural rigidity of the lithosphere allows compensation of the sedimentary load beyond the zone of stretching allowing downward flexing of the lithosphere beyond the stretched zone. Since the active rift phase is usually associated with a severe thermal perturbation the flexural rigidity of the lithosphere is expected to be very low during active rifting. However cooling attendent with sag pahse subsidence will increase the flexural rigidity causing the loading due to emplacement of sediment to be compensated on length scales which increase with time (Figure 10.3). White and McKenzie (1988) argue that the

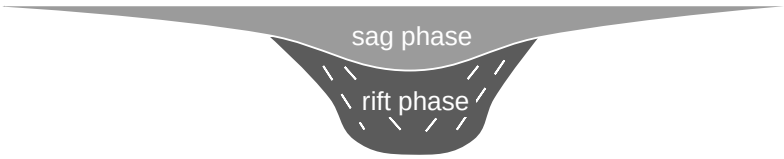

Figure 10.10: Schematic cross section showing characteristic steer's head formation of rift basins.

flexural rigidity of continental lithosphere is insufficient to explain the Steer's Head geometry and regard the characteristic geometry as a function of heterogeneous stretching of the lithosphere, with the characteristic length scale for mantle stretching greater than the length scale for crustal stretching. Indeed there is no good reason that stretching should be homogeneous on the scale of the lithsophere, and the resulting values of β_c and β_l (the reciprocals of f_c and $f_l - f_c$, respectively) are shown in Figure 10.3. This allows

subdivision of the basin into three regions which show characteristic elevation changes. Region a where the rift phase subsidence is greater than for homogeneous stretching; region b where the rift phase elevation change is either subsidence or uplift, but which show substantial sag phase sedimentation with sedimetation onlapping the basin margins progressively through the sag phase, and region c where there is only uplift during rifting and sag restores the initial elevation of the lithosphere (i.e., no net subsidence). The respective $f_l - f_c$ paths are shown in Figure 10.3.

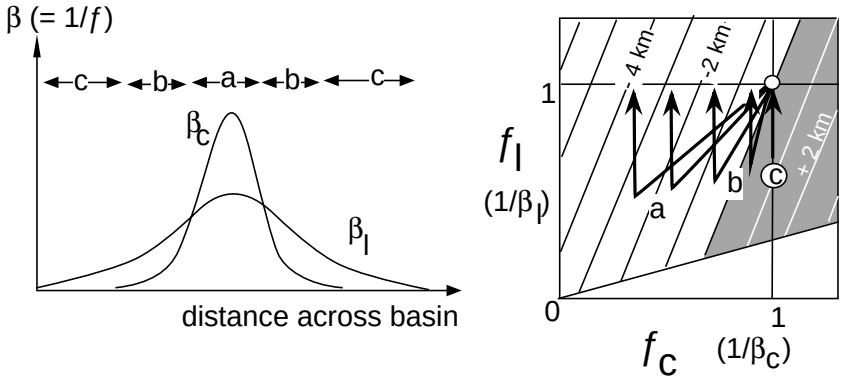

Figure 10.11: Heterogeneous stretching model for Steer's Head formation (after White and McKenzie, 1988). See text for discussion.

10.4 Topography of normal fault terrains

Rotation of normal fault blocks around horizontal axis is a necessary consequence of extension on a single set of domino faults (Figure 10.4). In the case where the normal faults are planar, rather than listric, it is easy to calculate the finite extension, β, from the dip slope, θ, as well as the observed orientation of the faults, α (Figure 10.4)

$$\beta = \frac{l_i}{l_o} = \frac{\sin(\theta + \alpha)}{\sin(\alpha)} \tag{10.17}$$

It is possible that the footwall escarpments may be emergent even though the isostatic considerations indicate extension produces over-

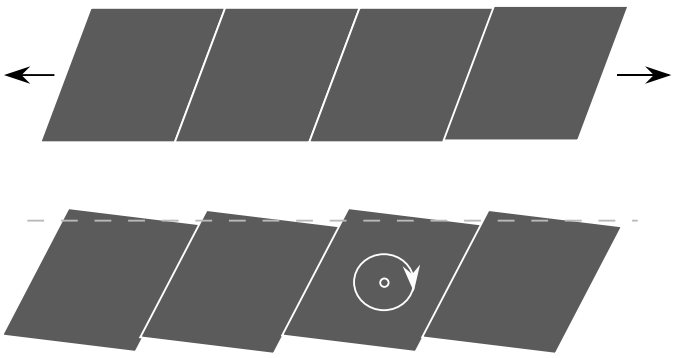

Figure 10.12: The deformation of planar faults forming a set of dominoes requires rotation about a horizontal axis in order that strain compatibility be maintained. Planar normal faults of this type root in a zone of pervasive aseismic deformation corresponding to the seismic-aseismic transition at around 10-15 km depth.

Figure 10.13: Schematic figure depicting the determination of the stretching factor from orientation of a domino fault system (see text for discussion).

all subsidence. The emergence of the footwall escarpments is due to the horizontal rotation component of tilting normal fault sets. Figure 10.4 shows schematically how the problem can be conceptualised.The rotation of the dip slopes can be understood as a rotation about a fulcrum. This is the point on the dip slope that in the absence of any isostatically induced subsidence would remain at constant elevation. In fact this fulcrum undergoes the calculated subsidence (S_i) for the appropriate extension, β. The condition for an emergent footwall escarpment is clearly that $\Delta H > S_i$. For a given amount of extension (i.e., fixed S_i), ΔH will be proportional to the horizontal spacing of the faults. Despite the common assertion that normal fault systems are listric (that is they curve to shallower orientations at depth), there is considerable debate amongst seismologists as to

Figure 10.14: See text for discussion

whether this is the case, with at least one vociferous group (McKenzie, Jackson etc.) arguing that normal fault sets are generally planar. In modern extensional fault systems normal faults tend to nucleate at around 60^o. With increased extension the fault sets rotate to shallower angles and seem to lock at around 30^o. Futher extension must be accommodated by the formation of a new set of steeply dipping (60^o) faults, which dissect an progressively rotate the older inactive set.